Sustainable Energy & Fuels

ROYAL SOCIETY OF CHEMISTRY

PAPER

View Article Online
View Journal

Cite this: DOI: 10.1039/d6se00062b

Life cycle assessment of perovskite solar cell manufacturing: effects of scale and process control

Nathan Dodd, *[a] Alan Dunbar, [a] David Bird, [b] Lenny Koh [c] and Rachael Rothman [a]

Semiconductors underpin many modern technologies, from data processing and displays to power generation, and their performance relies on precise thin-film deposition processes. These processes control the composition and interfaces between device layers, ensuring that semiconducting materials function reliably without degradation. In high-value devices such as perovskite solar cells, variations in deposition methods can significantly affect both material use and product quality. Improving the precision, consistency, and sustainability of thin-film deposition is therefore essential to enable scalable, efficient, and environmentally responsible manufacturing. This study employs a process-based Life Cycle Assessment (LCA), extended to include activity-level steps, to evaluate environmental impacts across laboratory- and pilot-scale perovskite solar cell production. The analysis highlights energy consumption in processing equipment and facility operations as the dominant environmental burden, with the deposition stage representing a key target for efficiency improvements. Scaling from laboratory to pilot-scale production reduces perovskite solar cell manufacturing costs by approximately 99.8% per m^2 of active area, with an additional ~8% reduction achieved through enhanced process control. At this scale, environmental impacts decrease by over 98% across global warming potential, human toxicity and aquatic ecotoxicity. Further integration of automated control systems lowers global warming and toxicity impacts by around 10%, while substituting grid electricity with low-carbon wind power amplifies these gains, reducing carbon emissions by up to 79%. The results demonstrate that combining process optimization with renewable energy sourcing provides a clear pathway toward sustainable, scalable perovskite solar cell manufacturing. The methodology is also broadly applicable to other thin-film semiconductor processes, offering guidance for improving operational efficiency while minimizing environmental impact.

Received 16th January 2026
Accepted 8th May 2026

DOI: 10.1039/d6se00062b

rsc.li/sustainable-energy

1 Introduction

Photovoltaic (PV) devices contain thin layers of semiconductors that have the ability to absorb solar radiation and convert it into electrical energy. When sunlight is absorbed by a semiconductor, energy is transferred to electrons increasing their electrical potential energy and enabling them to move freely. This movement of electrons generates an electric current, a phenomenon known as the photovoltaic effect.

Most conventional photovoltaic devices are made from silicon. However, recent research has focused on alternative materials, including a promising class of compounds known as perovskites. Perovskite solar cells (PSCs) offer high efficiency at low cost, driving their rapid adoption in photovoltaics.[1]

Initial investigations into perovskite materials for solar energy conversion began in 2009, with early devices demonstrating modest power conversion efficiencies of approximately 3.8%.[2] Since then, rapid advancements in material design and device architecture have significantly improved performance. Laboratory-scale PSCs have now achieved efficiencies exceeding 27% and when integrated with silicon in tandem configurations, these devices have reached efficiencies of over 34%.[3] This highlights their potential as a highly efficient and cost-effective solar technology.

1.1 Perovskite solar cells

PSCs are constructed as a series of thin layers, each with a defined role in device operation as per Table 1 alongside examples of materials for each layer. Various studies detail various similar fabrication processes and device architectures.[4–6] At the base lies the substrate, typically glass or a flexible polymer, which provides mechanical support and, in most cases, allows light to pass through. On top of this sits the transparent electrode which both conducts charge and admits incoming light.

[a]The University of Sheffield School of Chemical, Materials & Biological Engineering, Mappin Street, Sheffield, S1 3JD, UK. E-mail: iamndodd@gmail.com

[b]CPI, The Neville Hamlin Building, Thomas Wright Way, Sedgefield, County Durham, TS21 3FG, UK

[c]The University of Sheffield Management School, Conduit Road, Sheffield S10 1FL, UK

Table 1 Functional layers and typical materials in a perovskite solar cell device

Layer	Description	Typical materials
Substrate	Base that supports all layers; usually transparent to let light through	Glass, plastic (for flexible devices)
Transparent electrode (front contact)	Conductive layer that allows light to enter while collecting electrons or holes	Indium Tin Oxide (ITO), Fluorine-doped Tin Oxide (FTO)
Hole Transport Layer (HTL)	Moves holes to the electrode and blocks electrons	Spiro-OMeTAD, PTAA, PEDOT:PSS, NiO_x
Perovskite layer	Absorbs sunlight and generates electrons and holes	$CH_3NH_3PbI_3$, $CsPbI_3$, $FA_{0.85}MA_{0.15}Pb(I_{1-x}Br_x)_3$
Electron Transport Layer (ETL)	Moves electrons to the electrode and blocks holes	TiO_2, SnO_2, PCBM
Buffer or interfacial layer	Improves contact between layers, reduces energy losses, and enhances stability	PCBM, LiF, ZnO, C_{60}, MoO_x, or insulating polymers like PMMA
Metal electrode (back contact)	Final electrode that collects charges; usually a metal layer	Gold (Au), Silver (Ag), Aluminum (Al), carbon paste
Encapsulation layer	Protects the device from moisture, oxygen, and mechanical damage	Glass, UV-curable resin, barrier films

Charge-selective layers then flank the perovskite absorber: the hole transport layer extracts holes, while the electron transport layer extracts electrons. The central perovskite layer itself is the active light absorbing material, typically composed of lead halide perovskites. Additional buffer or interfacial layers are often included to optimise the electrical contact between layers and suppress recombination. Finally, a metal electrode serves as the back contact, and an encapsulation layer provides physical and chemical protection.

1.2 Solar cell manufacturing

Manufacturing can be understood across three levels: lab scale, which focuses on innovation and discovery; pilot scale, which aims to produce consistent material and sufficient quantities for real-world testing; and full-scale production, which prioritises minimising cost and maximising yield through operational efficiency.

The laboratory-based PSC is intentionally designed to maximize experimental flexibility and variation within a controlled environment. This approach facilitates the exploration of a wide range of models, design configurations, and material compositions, enabling researchers to test hypotheses, optimize parameters, and evaluate novel concepts efficiently. The primary focus is on versatility and adaptability rather than production throughput or cost efficiency, which is critical for advancing fundamental understanding and innovation.

Conversely, the pilot-scale architecture is engineered with a focus on economic and operational efficiency, targeting the validation of a streamlined production process intended for scale-up. This system is optimized to produce a single, standardized formulation or "recipe" at higher volumes, minimizing variability to ensure consistent product quality, reduce waste, and lower production costs. The pilot-scale setup embodies principles aligned with industrial manufacturing, where repeatability and cost effectiveness are paramount. This focus necessitates a more rigid and specialized system design that prioritizes throughput and efficiency over the experimental flexibility characteristic of laboratory settings.

The divergence between these two architectures stems from their contrasting purposes: the laboratory PSC prioritizes experimental breadth and adaptability to accommodate diverse research goals, whereas the pilot-scale system emphasizes scalability, economic viability, and process stabilization. Understanding these distinctions is crucial for interpreting performance data, scaling results, and developing appropriate lifecycle and sustainability assessments tailored to each context.

Tian *et al.*[7] highlights the critical role of durability in enhancing the life cycle sustainability of perovskite architectures. The current focus in perovskite PV research and industry has accordingly shifted from maximizing efficiency to improving stability. Perovskite solar cells are highly sensitive to moisture, oxygen, and UV exposure, which cause degradation of the perovskite layer.[8]

Recent life cycle assessments (LCAs) on PSCs have underscored the critical importance of manufacturing efficiency, particularly in the deposition and processing stages.[9] PSCs have rapidly advanced over the past decade, but scalability remains a key challenge as many deposition methods have been tested only at laboratory scale.[10] Common deposition methods include spin coating, slot-die coating, blade coating, thermal evaporation, sputtering, chemical vapor deposition (CVD), and atomic layer deposition (ALD). Solution-based fabrication methods such as spray coating show significantly lower energy use and carbon emissions than vapor-based approaches, while roll-to-roll production offers the lowest overall life cycle impacts.[11]

Research by Celik *et al.*[12] on vacuum, solution, and HTL-free perovskite solar cell devices suggests an energy payback time in the region of 1 to 1.5 years. This research also considered the differences between common laboratory-scale deposition techniques, such as spin coating and large-scale manufacturing methods. They noted that spin coating results in substantial material loss, with approximately 90% of the precursor solution not incorporated into the active layer. Such inefficiencies pose challenges for large-scale production and underscore the need for alternative methods. A study by Wong-Stringer[13] identified

that the next critical step is to demonstrate scalable fabrication processes capable of producing modules with significantly larger active areas. Considerable effort is still ongoing in this area.[14]

1.3 Spin coating deposition

Spin coating is a low cost, facile method of depositing layers onto a substrate. This makes the process ideal for lab scale initiatives, such as Zhang *et al.*[15] However, the process faces severe limitations in scalability, making commercialization challenging. The deposition effectiveness, which describes how much material remains on the substrate during the spinning process[16] is governed by the viscosity of the precursor inks. In spin coating, low-viscosity inks are easily flung off the substrate due to centrifugal forces, resulting in significant material waste and low deposition efficiency. Conversely, inks with higher viscosity tend to exhibit improved retention, leading to thicker and more uniform films.[17]

The viscosity of the precursor solution, the spin-coating rotation speed and the duration are critical parameters that govern the uniformity, thickness, and surface morphology of spin coated thin films.[18] Masruroh *et al.*[19] state that higher solution viscosity tends to increase film thickness and roughness, while longer spin times promote thinner, smoother, and more uniform layers. Each spin-coating parameter influences material waste, with higher solution viscosity leading to greater losses during the coating process, as well as directly influencing the performance and efficiency of devices.

1.4 Screen printing deposition

Screen printing deposition is a fabrication technique in which a patterned mesh screen serves as a stencil to selectively transfer inks or pastes onto a substrate. The ink is forced through the open areas of the mesh by means of a squeegee, resulting in the deposition of a controlled material layer with a predefined pattern.[20,21]

The primary advantages of screen printing include its cost effectiveness and scalability, making it well suited for large area, high throughput manufacturing processes.[22] Additionally, it allows for direct patterning without the need for subsequent lithographic steps, thereby simplifying the fabrication workflow.

Screen printing is also compatible with a diverse range of ink formulations, including conductive, semiconductive, and insulating materials. Furthermore, the thickness of the deposited layer can be modulated through variations in mesh size and ink viscosity, offering a degree of process flexibility. This is because screen meshes have hole sizes on the order of hundreds of microns, enabling the use of particulate dispersions containing, for example, 50-micron metallic flakes. Larger particles create longer and more continuous conductive pathways, improving conductivity, while also allowing the deposition of much thicker films.

However, the technique exhibits certain limitations. The achievable resolution is relatively coarse compared to alternative methods such as photolithography or inkjet printing, which may restrict its application in devices requiring fine patterning.[10] Deposited layers often exhibit increased surface roughness, which can negatively impact device performance and reliability. This effect is driven by the materials used (*e.g.*, very large flakes) rather than the deposition method. If the same materials were spin-coated, the surface would likely be even rougher because the process lacks meniscus-driven levelling.

Additionally, material waste can be significant due to excess ink usage and cleaning requirements, potentially affecting the overall sustainability of the process. Finally, screen printing demands stringent control over ink rheology and substrate surface properties to ensure uniform layer formation, which introduces process sensitivity.

1.5 Slot die coating

Slot-die coating is a precise and high throughput technique for depositing liquid films onto flat substrates or continuous rolls of material.[23] It is widely used in industrial settings due to its ability to deliver highly controlled film thickness, governed primarily by the slot gap and the material flow rate. These parameters can be readily adjusted, allowing the method to accommodate a wide range of formulations. The technique is also highly material efficient, particularly in roll-to-roll processing, where coating can be closely matched to the required geometry, minimising waste.

The method is most suited to large-scale production, as its primary limitation arises from the need to fill the internal volume of the coating head and delivery system before deposition can begin. This requires a minimum volume of material, typically on the order of tens of millilitres, which can be prohibitive when working with expensive, research-grade materials in laboratory settings.[24]

Slot-die coating also offers flexibility in deposition width and patterning. Coating width can be adjusted using interchangeable shims, and multiple stripes can be deposited simultaneously through multi-slot configurations. In the context of solar cell manufacturing, this enables the parallel fabrication of multiple devices on a single substrate, which can subsequently be separated into individual cells or interconnected to form modules.

1.6 Environmental impacts of manufacturing methods

This study focuses on two contrasting manufacturing methods: spin coating, which is widely used at laboratory scale for research and device development, and screen printing, which is more representative of pilot-scale manufacturing. Together, these methods capture the transition from highly flexible, research-oriented processing to more scalable and material-efficient production approaches. A broad body of literature has examined a range of deposition techniques under different research objectives; studies that specifically address spin coating, screen printing, and the challenges associated with scaling up perovskite device fabrication are reviewed in this section.

A previous cradle-to-gate LCA demonstrates that inkjet-printed PSCs significantly reduced global warming and energy

demand by an order of magnitude compared to spin coating.[10] The study finds that inkjet-printing is 36% less in energy intensive than spin coating and reaffirms the challenges of spin coating due to 95% of the ink being wasted in this case.

A study by Espinosa *et al.*[25] considers two different methods for making perovskite solar cells based on laboratory synthesis from previous research, with vapour-deposited cells reaching 15.4% efficiency and spin-coated cells 11.5%. This demonstrates that both the fabrication method and the cell design strongly influence photovoltaic performance. Life cycle assessment at laboratory scale indicates that the carbon footprint of perovskite solar cells is higher than similarly scaled organic photovoltaic devices, with vapour deposition producing 366 g CO_2 per kWh and spin coating producing 350 g CO_2 per kWh. Espinosa *et al.*[25] suggests that this is mainly due to high electricity consumption during manufacturing. Both fabrication methods experience significant material losses, with around 70% lost during vapour deposition and 90% lost during spin coating.

Future development of more sustainable PSCs will benefit from integrated life cycle assessment and supply chain environmental profiling, alongside strategies for recyclability and improved stability. Addressing encapsulation, flexible substrates, and scalable deposition methods will be essential for transitioning PSCs from laboratory prototypes to commercially viable photovoltaic technologies.[26,27]

1.7 Knowledge gap

Several knowledge gaps emerge from the current understanding of deposition processes in thin-film and perovskite solar cell manufacturing. First, despite the recognized importance of deposition methods on material use and film quality, there is limited quantitative understanding of how specific process variations such as precursor viscosity, deposition speed, and layer uniformity directly influence both device performance and material efficiency at scale.

Second, while automated control systems have been proposed to stabilize deposition conditions, there is a lack of experimental data demonstrating their effectiveness across different deposition techniques and scales, particularly in terms of reducing material waste and achieving reproducible film properties.

Third, environmental assessments remain incomplete: life cycle assessment studies often focus on laboratory-scale processes, leaving uncertainties about how that knowledge would translate to pilot or industrial scale deposition processes and affect energy consumption, material losses, and overall environmental impact.

Finally, the integration of process control with sustainability assessment remains underexplored, limiting understanding of how automation and monitoring can simultaneously improve operational efficiency and environmental performance. Addressing this gap is essential for enabling scalable, reproducible, and sustainable manufacturing of perovskite solar cells. Moreover, the methodology developed here is transferable to a broad range of semiconductor technologies. Its ability to capture both process-level parameters and facility-scale impacts means it can be applied to alternative deposition methods, device architectures, and manufacturing environments. Future work should therefore extend this framework to additional processes and product types, providing wider insight into how scaling, material choices, and operational strategies influence environmental outcomes across the semiconductor sector.

2 Methodology

2.1 LCA methodology

The data flow architecture, depicted in Fig. 1, demonstrates the structured and systematic framework used for modelling manufacturing scenarios through an integrated life cycle inventory (LCI) approach. This framework facilitates the linkage of diverse input data sources, sequential processing stages, and output metrics, thereby supporting comprehensive analyses that encompass temporal, economic, and environmental dimensions. However, the effectiveness of this approach depends heavily on data quality and system boundaries, issues that must be carefully managed to ensure robust and meaningful results.

This activity-focused approach can be seen as an extension of traditional process-based LCA, shifting the emphasis from aggregated unit processes to discrete operational steps within manufacturing. This method also allows more precise scenario analysis, such as evaluating the effects of alternative deposition techniques, equipment choices, or energy sources, making it particularly useful for emerging technologies like perovskite solar cells where process-level improvements can substantially influence overall sustainability.

2.1.1 Impact category selection. This study evaluates the environmental impacts of perovskite solar cell production using a focused subset of midpoint indicators from the ReCiPe 2016 life cycle impact assessment method. Given the study's emphasis on the manufacturing stage, rather than device use or end-of-life, a targeted selection of impact categories has been made to reflect the most relevant processes and environmental concerns associated with laboratory and early industrial-scale fabrication. The selected categories include global warming potential, total human toxicity, total aquatic ecotoxicity, and mineral resource scarcity. Global warming potential, expressed in kilograms of CO_2-equivalents, reflects the climate change impact of manufacturing. Processes such as thermal annealing, vacuum deposition, and substrate treatment involve substantial electricity use, particularly from fossil-based sources, making it important to minimize emissions to ensure net-positive benefits over the device life cycle. Total human toxicity, combines carcinogenic and non-carcinogenic impacts to provide an integrated indicator of potential harm to human health. Major contributors include solvents such as DMF and DMSO and heavy metals like lead iodide, and combining the impacts offers a simplified overview for comparison. Total aquatic ecotoxicity aggregates freshwater and marine effects from potential chemical emissions to water bodies, while terrestrial ecotoxicity is excluded due to its limited relevance in controlled manufacturing environments. Mineral resource scarcity,

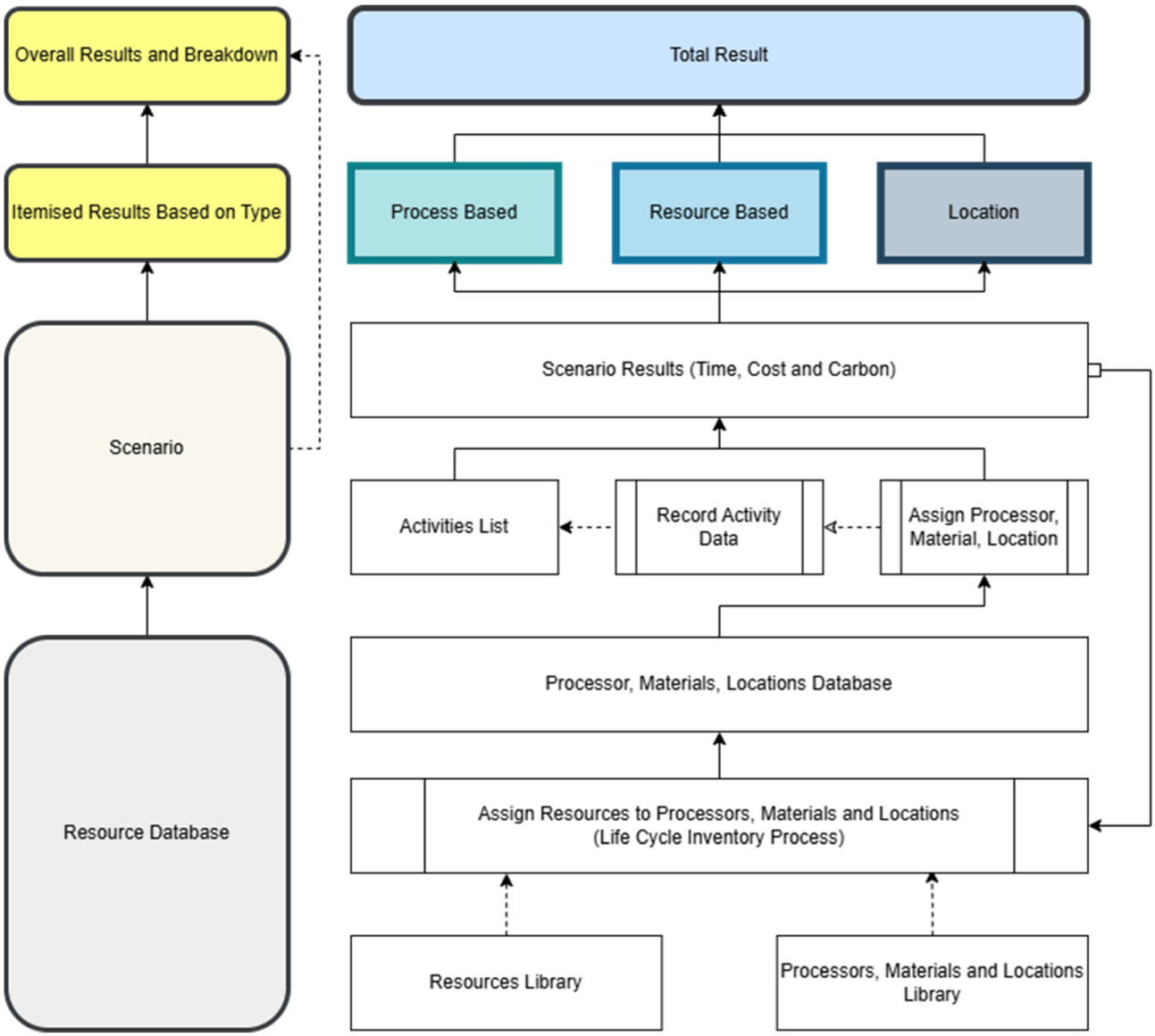

Fig. 1 Dynamic activity-based LCA data flow showing the iterative loop from scenario definition to activity modelling, LCI data integration, and labelled impact results.

reported in kg copper equivalents, indicates the energy and effort required to extract finite metals. Resource-intensive components such as gold, silver, or ITO can significantly influence this metric, highlighting considerations for long-term scalability. Other ReCiPe midpoint categories were excluded on the basis of low relevance, redundancy, or limited resolution at the considered scale.

2.1.2 Definition of study outputs. Embodied impacts refer to the environmental burdens from manufacturing, constructing, and installing the machinery, equipment, and facilities used in production, rather than the products themselves. These impacts include raw material extraction, processing, transport, and assembly. Since these assets are used repeatedly over extended periods, their impacts are allocated over their operational lifetimes, with each product or batch bearing a fraction proportional to its share of total usage.

Energy use in this study is exclusively electrical, covering equipment operation, environmental controls, lighting, and other essential infrastructure. Its environmental impact depends on the energy mix, equipment efficiency, and operational duration, making it a key factor in lifecycle assessments.

In this study, facilities embedded refers to the environmental impacts associated with the construction and material composition of buildings and infrastructure (*e.g.*, cleanroom structure, ventilation systems, and installed equipment), which are allocated over their operational lifetime. In contrast, facilities energy represents the operational energy demand required to run these environments, including electricity for lighting, heating, ventilation, and, in the case of pilot-scale production, cleanroom climate and air quality control.

Materials are classified in two ways. Functional materials become part of the final product, while lost or wasted materials

including evaporated solvents, discarded residues and consumables, do not contribute to the final product but still incur environmental impacts. Quantifying these losses is essential for evaluating the overall resource efficiency and identifying opportunities for process improvement.

2.2 Manufacturing scenario

The goal of this study is to evaluate and compare the environmental performance of laboratory-scale and pilot-scale perovskite solar cell (PSC) manufacturing systems, with a focus on identifying key factors influencing sustainability and production efficiency. The functional unit is defined as 1 m^2 of active perovskite solar cell area, encompassing both active and inactive regions and accounting for defective units requiring additional production.

The study scope covers the complete production process for perovskite cells fabricated on glass substrates *via* wet film deposition, maintaining uniform layer architectures across scales. Environmental impacts are assessed using consistent life cycle inventory (LCI) data and databases. Supply chain variability is excluded. The system boundary includes all relevant material, energy, and equipment inputs for cell fabrication, with deposition methodology representing the primary process distinction between scales. A laboratory environment and an industrial pilot-scale environment are investigated. Table 2 provides further details of the different device production scenarios.

2.2.1 Device layer thickness. A single consistent set of materials is employed across both production methods, with uniform layer thicknesses maintained for each material in every device (see Table 3). This deliberate standardization serves to isolate and emphasize the differences inherent in the production architectures themselves, rather than conflating variability arising from material composition or device design. By controlling material inputs and structural parameters, the analysis can focus more precisely on the operational characteristics, efficiencies, and environmental impacts associated with the distinct manufacturing machines and processes utilized in each method.

This approach ensures that observed differences in performance or sustainability metrics are attributable primarily to the manufacturing pathways rather than variations in product chemistry or design intricacies. Consequently, the study can more effectively evaluate the relative advantages and limitations of the production systems, providing clearer insights into process optimization and resource utilization. Such controlled experimental design is essential for developing robust comparative assessments that inform both process improvement and lifecycle impact evaluations within the broader context of manufacturing sustainability.

Table 3 Thickness of layer used for all cell architectures

Material	Thickness (nm)
ITO	100
SnO_2	20
Perovskite	400
Spiro-OMeTAD	250
Ag	100

2.2.2 Lab scale device architecture and manufacturing set-up. Precise data on layer thicknesses, combined with input from academic and industry experts, were used to quantify the material requirements for pilot-scale fabrication of perovskite solar cells. These thicknesses provide the basis for calculating the volume and mass of materials deposited at each stage of fabrication. Expert guidance further refined the estimates by accounting for practical factors such as material utilization efficiency, deposition losses, and scaling effects observed when moving from laboratory to pilot production. The materials required for each layer are presented in the accompanying Table 4. The inventory encompasses all relevant material and energy inputs, along with emissions and infrastructure contributions associated with the fabrication of a single device. Data were compiled from technical information provided by academic and industry experts and selected based on the components available in the ecoinvent database. Where direct data were unavailable, assumptions based on equipment specifications and process rates were used to approximate contributions.

The fabrication steps are listed in Table 5. The process begins with substrate cleaning and preparation, which involves handling the substrates and performing ultrasonic cleaning using surfactant, acetone, isopropanol (IPA), and water. The water is heated as needed using a kettle, and substrates undergo oxygen plasma cleaning to ensure surface readiness. Following substrate preparation, inks are formulated by mixing SnO_2 nanoparticle suspension with water, which is then sonicated to disperse any aggregates. Perovskite ink is prepared by combining lead iodide, methylammonium iodide (MAI), and

Table 2 Comparison of lab-scale and pilot-scale perovskite solar cell features and manufacturing methods

Feature	Lab scale	Pilot scale
Substrate size	15 mm × 20 mm = 300 mm^2	203.2 mm × 203.2 mm = 41 290.24 mm^2
Pixel/cell count	8 pixels	30 cells
Pixel/cell size	1.6 mm × 1.6 mm	10 mm × 80 mm
Active area per substrate	1.6 × 1.6 × 8 = 20.48 mm^2	10 × 80 × 30 = 24 000 mm^2
Active area ratio	6.83%	58.13%
Deposition method	Spin coating (manual, sequential layers)	Slot-die coating, screen printing (continuous/layered)
Interconnection	Manual, individual probing	Integrated: parallel/series layouts
Production style	Manual, research-scale	Semi-automated, pilot-line
Use case	Material screening, cell design testing	Scalable fabrication, yield testing, device prototyping

Table 4 Core material components of a laboratory-scale perovskite solar cell, limited to materials incorporated in the final device and excluding auxiliary inputs used during manufacturing (*e.g.*, cleaning water) (blue is used to denote inputs, red is used to denote wastes)

Modelled sub component	Material components of PSC		
Patterned ITO on glass	Ecoinvent data selection	1.00	Unit
Glass	Solar glass, low-iron {GLO}	0.825	g
Glass waste	Waste packaging glass, unsorted {GLO}	1.05	g
Indium tin oxide	Indium tin oxide powder, nanoscale, for sputtering target {RER}	0.214	mg
SnO_2 ink	Ecoinvent data selection	1.35	µL
Isopropanol	Isopropanol {RER}	1080	µg
Tin oxide	Tin {GLO}	210.6	µg
	Tap water {Europe without Switzerland}	270	µg
Process waste	Waste, from silicon wafer production, inorganic {GLO}	1560.6	µg
Perovskite ink	Ecoinvent data selection	1.50	µL
DMF dimethylformamide	Dimethylamine {RER}	9	µg
	Methyl formate {GLO}	9	µg
	Electricity, low voltage {GB}	25.98	µWh
Lead chloride	Lead concentrate {GLO}	4.47	µg
	Chlorine, gaseous {RER}	1.53	µg
	Electricity, low voltage {GB}	2.31	µWh
Lead iodide	Iodine {GLO}	3	µg
	Potassium hydroxide {GLO}	1.5	µg
	Nitric acid, without water, in 50% solution state {RER w/o RU}	6	µg
	Lead concentrate {GLO}	3	µg
	Electricity, low voltage {GB}	1.38	µWh
Methylammonium iodide	Methylamine {RER}	6	µg
	Hydrogen, gaseous {GLO}	6	µg
	Electricity, low voltage {GB}	6.12	µWh
Process waste	Waste, from silicon wafer production, inorganic {GLO}	35850	µg
Spiro Ink	Ecoinvent data selection	1.35	µL
Acetonitrile	Acetone, liquid {RER}	0.0405	µg
Chlorobenzene	Monochlorobenzene {RER}	331.8	µg
LiTFSI	Lithium sulfate {GLO}	1.62×10^{-5}	µg
Spiro-OMeTAD	Methyl-3-methoxypropionate {GLO}	2.4	µg
Epoxy	Ecoinvent data selection	50.00	µL
Epoxy	Epoxy resin, liquid {RER}	49.5	mg
	Tap water {Europe without Switzerland}	5	mg
Silver (Ag)	Ecoinvent data selection	25.30	mg
Silver	Silver {GLO}	25.3	mg
Process waste	Waste, from silicon wafer production, inorganic {GLO}	25.3	mg
Encapsulation coverslip	Ecoinvent data selection	1.00	Unit
Glass	Solar glass, low-iron {GLO}	0.5	g
Glass waste	Waste packaging glass, unsorted {GLO}	0.25	g

dimethyl sulfoxide (DMSO), while spiro ink is also mixed alongside an ultrasonic cleaner.

Subsequently, the spin coating and layer deposition stage commences, where SnO_2 ink is spin coated onto the substrates, followed by heating and drying on a hotplate. The spin coater is cleaned after each layer is deposited to maintain process integrity. The perovskite ink is then spin coated with an anti-solvent added during spinning to enhance film quality, followed

Table 5 Key equipment and tools used in lab-scale perovskite device production by process step

Step	Equipment used
1. Substrate cleaning & preparation	Ultrasonic cleaner tool, kettle, plasma cleaner
2. Ink preparation	Ultrasonic cleaner tool
3. Spin coating & layer deposition	Spin coater, hotplate
4. Post-processing	Technician
5. Metal evaporation (Ag layer)	Vacuum pump, metal evaporator
6. Final assembly	UV curing box

by further heating and drying. Finally, the spiro ink is applied by spin coating. Excess material is wiped away after each layer to allow unhindered electrical connection to both the top and bottom contacts of the final devices.

Post-processing involves allowing the coated samples to air-dry overnight to stabilize the films. The metal evaporation step includes loading silver into a tungsten boat, evacuating the deposition chamber with a vacuum pump, and heating the source to deposit the metal layer. After deposition, the glass chamber is cleaned of any residual silver.

The process concludes with the final assembly stage, which entails selecting cover slips, applying epoxy to bond the cover glass, and curing the assembly within a UV curing box to complete the device encapsulation. Throughout these stages, the combination of technician support and specialized laboratory equipment ensures precise control and reproducibility.

Yield and defect rates are rarely reported for laboratory-scale perovskite fabrication, as the primary objective at this stage is the development of novel materials and device architectures rather than process optimisation. In contrast, higher-volume manufacturing studies report yields of up to ~96%,[28] providing a useful benchmark for well-controlled systems. Drawing on this, and supported by discussions with laboratory technicians and industry partners,[29] a defect rate of 20% is assumed for laboratory-scale processes. This reflects the inherent variability associated with manual handling, limited process control, and non-optimised equipment typical of experimental environments. The estimate is consistent with broader observations in early-stage photovoltaic fabrication and captures the inefficiencies commonly encountered in research scale production.[12]

2.2.3 Pilot scale device architecture and manufacturing set-up. The values in Table 6 were selected to represent the quantities of each component material in a single pilot-scale perovskite solar cell as described in Table 2. The inventory encompasses all relevant material and energy inputs, along with emissions and infrastructure contributions associated with the fabrication of a single device. Data were compiled from technical information provided by academic and industry experts and selected based on the components available in the ecoinvent database. Where direct data were unavailable, assumptions based on equipment specifications and process rates were used to approximate contributions. Pilot-scale production is conducted within a cleanroom to maximise yield and product quality by minimising defects caused by environmental dust and particles.

The manufacturing process summarised in Table 7 begins with substrate preparation, involving cleaning, rinsing, drying, and careful handling of glass substrates using equipment such as a 40 L ultrasonic bath, spin-cleaner, wash station, and a 115 L oven. This is followed by the deposition of the indium tin oxide (ITO) layer *via* sputtering, with key equipment including a 12″ planar sputter tool. Photolithography involves coating the substrates with photoresist, baking, UV exposure, developing, and plasma cleaning, utilizing a 12″ spin coater, hot plates, UV exposure tool, spin developer, and plasma cleaner to define the desired patterns. The etching stage removes parts of the ITO layer through acid etching, rinsing, drying, and microscopic inspection using a wet bench, wash station, oven, and compound microscope.

Ink formulation is then carried out by preparing SnO_2 and spiro inks, employing solvents and ultrasonic agitation with the help of technician tools and an ultrasonic cleaner. This stage remains broadly identical to the lab-scale scenario, as ink production is independent of both the deposition method and the manufacturing scale. Coating processes include slot-die coating of the SnO_2 and perovskite layers, followed by drying, heating, and edge cleaning, performed with an 8″ slot die coater, hot plates, and an edge-bead remover. Laser patterning shapes the coated substrates precisely using specialized laser patterning equipment. The final coating and handling stage applies the spiro ink, followed by overnight drying and cleaning of slot-die equipment. Metallization involves silver sputtering through a planar sputter tool, along with mask handling and inspection. Finally, the lamination and curing phase applies glue, laminates the device, performs UV curing, conducts a final inspection, and packs the finished product using automated glue robots, low-pressure chambers, and UV curing boxes.

A 5% defect rate is applied to the pilot-scale process, reflecting the increased reliability and uniformity of semi-automated deposition methods such as slot-die coating and screen printing, as recommended through discussion with industry[29] and in keeping with reported yield rates of 96% by Scarpulla *et al.*[28] These techniques offer improved control over film quality and reproducibility, reducing variability and material loss compared to manual lab-scale methods. The environmental impacts of human labour are excluded; while increased manual effort can improve yields at laboratory scale, this is not directly comparable to pilot-scale production without explicitly modelling inspection and rework.

2.2.4 Advanced control systems and alternative power source pilot studies. The control system in the pilot-with-

Table 6 Core material components of a pilot-scale perovskite solar cell, limited to materials incorporated in the final device and excluding auxiliary inputs used during manufacturing (*e.g.*, cleaning water) (blue is used to denote inputs, red is used to denote wastes)

Modelled sub component	Material components of PSC		
Glass substrate	Ecoinvent data selection	2.00	Unit
Glass	Solar glass, low-iron {GLO}	0.12	g
Glass waste	Waste packaging glass, unsorted {GLO}	0.00	g
SnO_2 ink	Ecoinvent data selection	0.48	µL
Isopropanol	Isopropanol {RER}	384.00	µg
Tin oxide	Tin {GLO}	74.88	µg
	Tap water {Europe without Switzerland}	96.00	µg
Process waste	Waste, from silicon wafer production, inorganic {GLO}	554.88	µg
Perovskite ink	Ecoinvent data selection	9.62	µL
DMF dimethylformamide	Dimethylamine {RER}	57.72	µg
	Methyl formate {GLO}	57.72	µg
	Electricity, low voltage {GB}	166.62	µWh
Lead chloride	Lead concentrate {GLO}	28.67	µg
	Chlorine, gaseous {RER}	9.81	µg
	Electricity, low voltage {GB}	14.81	µWh
Lead iodide	Iodine {GLO}	19.24	µg
	Potassium hydroxide {GLO}	9.62	µg
	Nitric acid, without water, in 50% solution state {RER w/o RU}	38.48	µg
	Lead concentrate {GLO}	19.24	µg
	Electricity, low voltage {GB}	8.85	µWh
Methylammonium iodide	Methylamine {RER}	38.48	µg
	Hydrogen, gaseous {GLO}	38.48	µg
	Electricity, low voltage {GB}	39.25	µWh
Process waste	Waste, from silicon wafer production, inorganic {GLO}	0.23	g
Spiro ink	Ecoinvent data selection	6.01	µL
Acetonitrile	Acetone, liquid {RER}	0.18	µg
Chlorobenzene	Monochlorobenzene {RER}	1477.12	µg
LiTFSI	Lithium sulfate {GLO}	0.00	µg
Spiro-OMeTAD	Methyl-3-methoxypropionate {GLO}	10.68	µg
Epoxy	Ecoinvent data selection	9.35	mL
Epoxy	Epoxy resin, liquid {RER}	9.26	g
	Tap water {Europe without Switzerland}	0.94	g
Silver (Ag)	Ecoinvent data selection	25.25	mg
Silver	Silver {GLO}	25.25	mg
Process waste	Waste, from silicon wafer production, inorganic {GLO}	25.25	mg
ITO etchant	Ecoinvent data selection	2.40	µL
Nitric acid	Nitric acid, without water, in 50% solution state {RER w/o RU}	3.31	mg
Process waste	Waste, from silicon wafer production, inorganic {GLO}	3.31	mg
ITO target	Ecoinvent data selection	27.00	mg
Sputtering target	Sputtering target, sintered, indium tin oxide {GLO}	27.00	mg
Process waste	Waste, from silicon wafer production, inorganic {GLO}	27.00	mg

control scenario is represented using a simplified life cycle inventory to capture the embodied impacts of camera, sensor, and PC-based monitoring equipment. These reflect work conducted concurrently in a laboratory environment. In the absence of a dedicated dataset for integrated control systems, 2 kg of electronics scrap {GLO} from ecoinvent was used as

Table 7 Key equipment and tools used in pilot-scale perovskite device production by process step

Process section	Key equipment used
1. Substrate preparation	40 L ultrasonic bath, spin-cleaner, 40 L wash station, 115 L oven
2. ITO deposition	12″ planar sputter tool, 4 point probe, film thickness tool
3. Photolithography	12″ spin coater, 12″ hot plates, UV exposure tool, spin developer, plasma cleaner
4. Etching	40 L wet bench (acid), 40 L wash station, 115 L oven, compound microscope
5. Ink formulation	Ultrasonic cleaner
6. Coating processes	8″ slot die coater, 12″ hot plates, edge-bead remover
7. Laser patterning	Laser patterning tool
8. Final coating & handling	Technician
9. Metallization	12″ planar sputter tool
10. Lamination & curing	Glue robot, low pressure chamber, UV curing box

a proxy to approximate the material and manufacturing burdens of these components. This conservative estimate represents the combined mass of key elements; sensors, cameras, processing units, and supporting electronics, while the end-of-life electronics dataset reasonably reflects their upstream material composition, dominated by metals, circuit boards, and semiconductors.

Although this approach introduces some uncertainty, the control system's contribution is small relative to operational energy and facility impacts, making the proxy sufficient to capture the order of magnitude of embodied impacts without affecting overall conclusions.

In addition, the system is assumed to operate with a continuous power demand of 100 watts, reflecting the consumption of energy for integrated sensing and data processing in pilot-scale environments. The defect rate is assumed to decrease from 5% in the standard pilot-scale scenario to 2% with the implementation of advanced automated control systems. This reduction should be understood as a hypothetical projection, intended to represent the expected improvements in process consistency and quality achievable through enhanced monitoring and control. The 2% value is not derived from a specific industrial dataset, but rather reflects a realistic, forward-looking estimate based on ongoing developments in automated manufacturing. In highly optimised production environments, defect rates of well below 1% are achievable, indicating that this assumption is conservative and appropriate for modelling incremental improvements rather than best-case performance. Layer deposition cycle times are halved under the control system scenario, but total production time is only slightly reduced by 2–3%, as other activities proceed at unchanged rates.

The study also evaluates the effect of sourcing electricity from a low-carbon system, using UK wind power (electricity, high voltage {GB}| electricity production, wind, >3 MW turbine, onshore) to align with the laboratory and pilot-scale datasets. Because energy use can be a major contributor to global warming impacts, shifting to renewable electricity has the potential to significantly reduce the environmental burden of this manufacturing scenario.

2.3 Key assumptions

Key modelling assumptions ensure consistent comparison across scenarios. A uniform device architecture and layer thickness are applied to isolate manufacturing effects from design variations. Defect rates of 20% (laboratory), 5% (pilot), and 2% (pilot with control) are assumed based on academic and industry input,[29] with defective units requiring full reprocessing. Facility and equipment impacts are allocated over their lifetimes according to throughput, while energy use is modelled as electricity consumption based on equipment specifications and process durations. Where primary data are unavailable, proxy datasets from ecoinvent (*e.g.*, electronics scrap for control systems) are used. Supply chain variability is excluded, and results are normalised to a functional unit of 1 m^2 of active area unless otherwise stated.

3 Results & discussion

The results are presented sequentially, beginning with the laboratory scale, followed by the pilot scale, the pilot system with advanced control, and finally the pilot system combined with wind-generated electricity. For each case, the analysis examines the overall environmental impacts, considering contributions from component materials, tool and equipment use, energy consumption, and facility-related demands such as cleanroom operation.

3.1 Lab scale PSC manufacturing

Table 8 summarises the environmental impacts and total cost for the laboratory-scale fabrication of a single perovskite solar device. Data are presented for key bill-of-materials (BOM) components, as well as process-related losses, energy consumption, and embodied equipment impacts. Environmental burdens are reported using ReCiPe 2016 midpoint indicators, specifically global warming potential, total human toxicity, total aquatic ecotoxicity, and mineral resource scarcity. Whilst the primary functional unit of this study is 1 m^2 of active perovskite area, the results initially presented in Table 8 are reported at the smallest practical production unit for laboratory-scale fabrication, corresponding to a single substrate containing 8 individual cells with a combined active area of 300 mm^2. These values reflect representative laboratory operating conditions and provide insight into the relative contributions of materials, processes, and facilities at low-throughput scale. The results are subsequently normalised and extrapolated to the 1 m^2 functional unit to enable consistent comparison across laboratory and pilot-scale manufacturing scenarios.

Table 8 Lab-scale environmental impacts associated with component materials incorporated into the final device, material losses during manufacturing and impacts from facility use, reported on a per-device basis (one substrate comprising 8 cells with a total area of 300 mm^2)

BOM	Estimated cost (£)	Global warming (kg CO_2-eq.)	Total human toxicity (kg 1,4-DCB-eq.)	Total aquatic ecotoxicity (kg 1,4-DCB-eq.)	Mineral scarcity (kg Cu-eq.)
Materials incorporated in the final device					
Ag	0.19	1.42×10^{-6}	1.60×10^{-4}	1.65×10^{-3}	1.71×10^{-8}
Encapsulation coverslip	0.64	5.40×10^{-4}	3.28×10^{-4}	3.22×10^{-5}	1.23×10^{-6}
Epoxy	0.23	2.40×10^{-4}	2.19×10^{-4}	2.36×10^{-5}	6.95×10^{-7}
Patterned ITO on glass	2.60	8.91×10^{-4}	5.42×10^{-4}	5.34×10^{-5}	2.04×10^{-6}
Perovskite ink	0.05	8.28×10^{-8}	5.65×10^{-7}	3.67×10^{-8}	3.15×10^{-9}
SnO_2 ink	0.00	6.30×10^{-10}	6.00×10^{-8}	1.72×10^{-7}	1.57×10^{-11}
Spiro ink	0.60	1.07×10^{-1}	7.15×10^{-9}	3.45×10^{-9}	3.50×10^{-13}
Materials lost & consumed					
Exclusive	38.35	4.65×10^{-2}	1.08×10^{-3}	6.43×10^{-2}	9.96×10^{-4}
Facilities & tool use energy					
Exclusive	1.65	1.74×10	4.01×10^{-4}	4.32×10^{-1}	4.65×10^{-3}
Facilities & tool embodied					
Exclusive	7.03	1.44×10	2.71×10^{-3}	3.51×10	9.00×10^{-2}
Production of device total					
Total of all elements	**51.33**	$\mathbf{3.22 \times 10}$	$\mathbf{4.25 \times 10^{-3}}$	$\mathbf{4.01 \times 10}$	$\mathbf{9.57 \times 10^{-2}}$

In the laboratory environment, material usage represents the primary contributor to overall production costs as shown in Fig. 2. This is particularly influenced by the spin coating deposition method, which is inherently wasteful due to low material retention and high overspray, necessitating excess quantities of expensive precursors. Across all considered environmental impact categories, embodied emissions, those associated with the production and maintenance of equipment and facilities, emerge as the dominant source of environmental burden. This is largely attributable to the small quantities of material used and the inherently slow nature of laboratory-scale processes, which result in disproportionately high usage times for energy-intensive equipment and infrastructure. Consequently, process duration, and by extension equipment occupancy time, is a critical factor in driving environmental impacts at the lab scale.

Table 9 presents the aggregated life cycle impacts associated with the production of 1 m^2 of active perovskite solar cell area, incorporating a 20% defect rate to reflect typical lab-scale manufacturing yield losses. The results are divided into three primary contributors: energy use during processing, embodied emissions from infrastructure and equipment, and all material inputs. Despite relatively modest environmental contributions, material costs dominate the total financial burden. In contrast, embodied and energy-related emissions are the principal drivers of global warming potential and resource scarcity, highlighting the environmental trade-offs inherent in current small-scale production approaches.

The cost breakdown for laboratory-scale perovskite cell fabrication is dominated by the material inputs, particularly specialty chemicals. The majority of the cost is attributed to Spiro-OMeTAD ink (73.9%), as seen in Fig. 3, reflecting its high unit price and the relatively large quantity required for device fabrication. Other significant cost contributors include the patterned ITO glass substrate and perovskite precursor ink.

Contributions from facilities and energy usage are comparatively negligible at this scale. The materials cost per total substrate produced (including both functional and defective units) is approximately £26.33. This figure accounts for all materials consumed during production, reflecting the

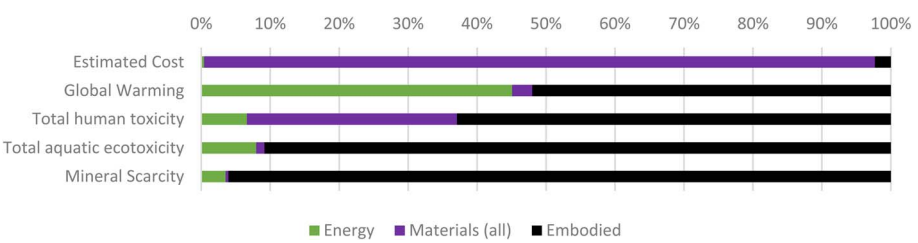

Fig. 2 Breakdown of environmental impacts by energy, materials, and embedded contributions for lab-scale manufacturing of perovskite solar cells.

Table 9 Breakdown of environmental impacts for lab-scale production of 1 m^2 active-area perovskite devices by category: energy, embodied facilities/tools, and materials

Category	Estimated cost (£)	Global warming (kg CO_2-eq.)	Human toxicity (kg 1,4-DCB-eq.)	Aquatic ecotoxicity (kg 1,4-DCB-eq.)	Mineral scarcity (kg Cu-eq.)
Energy (all sources)	£6833	7210	1.65	1690	19.3
Embodied (facilities & tools)	£38 207	8320	15.4	9010	523
Materials (all)	£1 607 322	466	7.64	271	2.24
Total impact	£1 652 362	15 995	24.65	10 972	544.37

inefficiencies and material losses typical in early-stage fabrication. The cost is not unrealistic given the use of expensive materials such as Spiro-OMeTAD and perovskite precursors, which are often purchased in small volumes at premium prices in laboratory contexts. This result highlights the economic challenges of low-throughput, high-defect-rate processes and underscores the potential for significant cost reductions through improved yield and scale-up.

The global warming impacts are primarily driven by infrastructure-related emissions and energy-intensive equipment. Facilities-embedded impacts account for 51.6% of the total, while equipment such as vacuum pumps (26.5%) and metal evaporators (6.1%) are also notable contributors due to their high energy demands and slow processing. Material contributions, such as DMF solvent, are minor by comparison but still measurable.

Human toxicity impacts are largely associated with the materials used, particularly silver (24.5%), which carries a significant toxicological burden despite its low mass contribution owing to background mining operations in the production silver. Facilities embedded emissions remain the dominant source (62.6%), while additional minor contributions arise from solvents and certain processing tools, such as vacuum pumps and evaporators.

Aquatic ecotoxicity is overwhelmingly influenced by the facilities' embedded impacts, which contribute 90.5% of the total. This is due to high copper usage associated with the building construction within the ecoinvent dataset. Equipment such as vacuum pumps and metal evaporators also contribute modestly. Material-related contributions, including those from silver and solvents, are present but comparatively small.

The mineral resource scarcity impact is heavily concentrated in the embodied emissions of facility infrastructure (95.1%) which is again a result of high copper usage associated with the building construction. Among individual tools, the vacuum pump, hotplate, and metal evaporator are the leading contributors, though their impacts are minor relative to infrastructure.

3.2 Pilot scale PSC manufacturing

Table 10 presents the estimated material and energy inputs, associated environmental impacts, and total cost for the production of a single perovskite solar device at the pilot scale.

Fig. 3 Proportional contributions of materials, processes, and facility use to environmental impacts in lab-scale perovskite solar cell manufacturing.

Table 10 Pilot-scale environmental impacts associated with component materials incorporated into the final device, material losses during manufacturing and impacts from facility use, reported on a per-device basis (one substrate comprising 30 cells with a total area of 41 290.24 mm^2)

BOM item	Estimated cost (£)	Global warming (g CO_2-eq.)	Human toxicity (mg 1,4-DCB-eq.)	Aquatic ecotoxicity (mg 1,4-DCB-eq.)	Mineral scarcity (mg Cu-eq.)
Materials incorporated in the final device					
Ag	0.19	1.4	52.6	1650	17.1
Epoxy CPI	4.68	44.9	30.6	4420	130
Glass substrate	20.00	128	29.1	7620	292
ITO etchant	0.00	0	0	0	0
Perovskite ink	0.29	0.53	0.67	0.24	0.020
SnO_2 ink	0.00	0.0002	3.5	0.061	0.0056
Spiro ink	2.67	0.0005	24.9	0.015	0.0016
Materials lost & consumed					
Exclusive	60.25	164	324	19 500	787
Facilities & tool use energy					
Exclusive	20.44	21 600	4530	2 730 000	57 800
Facilities & tool embodied					
Exclusive	270.56	2500	3000	1 370 000	107 000
Production of device total					
Total of all elements	**379.08**	**24.4 kg**	**8.0 kg**	**4.1 kg**	**0.17 kg**

Impact values are reported across four midpoint indicators, global warming potential, human toxicity, aquatic ecotoxicity, and mineral resource scarcity, using ReCiPe 2016 characterisation factors. The data reflect both direct bill-of-materials (BOM) components and upstream contributions from energy use and equipment embodiment. Whilst the primary functional unit of this study is 1 m^2 of active perovskite area, the results initially presented in Table 10 are reported at the smallest practical production unit for pilot-scale fabrication, corresponding to a single substrate containing 30 individual cells with a combined active area of 41 290.24 mm^2. These values reflect representative pilot scale operating conditions and provide insight into the relative contributions of materials, processes, and facilities at low-throughput scale. The results are subsequently normalised and extrapolated to the 1 m^2 functional unit to enable consistent comparison across laboratory and pilot-scale manufacturing scenarios.

The total environmental impacts associated with the pilot manufacturing process amount to 178.26 kg CO_2-equivalents for global warming, 0.07 kg 1,4-dichlorobenzene equivalents for total aquatic ecotoxicity, 54.30 kg 1,4-dichlorobenzene equivalents for total human toxicity, and 1.05 kg copper equivalents for mineral resource scarcity, based on a production cost of £3669.60 for 1 m^2 of active area.

A substantial portion of the financial cost associated with the pilot-scale manufacturing process arises from the materials required and the overhead costs linked to operating within cleanroom facilities (Fig. 4). Cleanrooms are essential to achieving high yield, as environmental dust can compromise device quality. In contrast, the majority of the global warming potential is attributable to energy consumption, reflecting the energy-intensive nature of precision fabrication techniques. While materials contribute less significantly to climate-related impacts, they play a more prominent role in human toxicity, largely due to the specific chemical compositions involved in perovskite device fabrication, including heavy metals and organic solvents. The impact category of mineral resource scarcity is primarily influenced by embodied emissions, which account for the upstream environmental burdens associated with the production of equipment and infrastructure due to the greater use of heavy metals and mining operations therein. These impacts are normalised according to

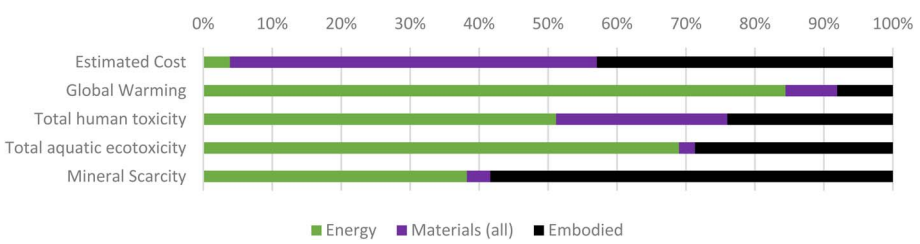

Fig. 4 Breakdown of environmental impacts by energy, materials, and embedded contributions for pilot-scale manufacturing of perovskite solar cells.

Table 11 Breakdown of environmental impacts for pilot-scale production of 1 m^2 active-area perovskite devices by category: energy, embodied facilities/tools, and materials

Category	Estimated cost (£)	Global warming (kg CO_2-eq.)	Human toxicity (kg 1,4-DCB-eq.)	Aquatic ecotoxicity (kg 1,4-DCB-eq.)	Mineral scarcity (kg Cu-eq.)
Energy (all sources)	£142.62	150.53	0.03	37.46	0.40
Embodied (facilities & tools)	£1575.08	14.39	0.02	15.57	0.62
Materials (all)	£1951.91	13.34	0.02	1.27	0.04
Total impact	£3669.61	178.26	0.07	54.30	1.06

expected tool lifetimes and usage intensity, highlighting the long-term resource demands embedded within capital assets.

Table 11 notes key cost and environmental impact metrics for pilot-scale production of 1 m^2 of active area perovskite device. Notably, pilot-scale results show significant reductions across all categories. For example, energy costs decrease from £6833 at lab scale to £142.62, while associated global warming emissions drop from 7210 to 150.53 kg CO_2-eq. Similar reductions are observed for human toxicity, aquatic ecotoxicity, and mineral scarcity impacts. Embodied impacts and material costs also decline substantially, reflecting improved efficiencies and economies of scale at pilot scale.

The results in Fig. 5 shows that the glass substrate is the single largest cost contributor at 24.5%, followed by Spiro ink (6.8%), water (6.5%), and epoxy encapsulant (5.7%). Facilities-related costs dominate overall, with embedded infrastructure accounting for 34.6% and energy use 2.4%, reflecting the high capital requirements of cleanroom operations. The substantial reduction in Spiro ink costs from lab to pilot scale arises from replacing spin coating with screen printing, which greatly reduces material waste and therefore the amount of ink required per layer.

Global warming impacts are mainly driven by energy consumption, with facilities energy contributing 55.1% of total CO_2-equivalent emissions. Among individual tools, 12″ hot plates are the largest contributor (18.6%), followed by the planar sputter tool (4.8%), glass substrate (3.2%), and 115 L oven (3.1%), indicating that process heat and vacuum systems are major sources of climate-related impacts due to high energy demands.

Human toxicity is dominated by facilities energy (32.7%) and embedded infrastructure (21.0%), with hot plates (12.3%), silver deposition (12.0%), and photoresist use (7.6%) also contributing substantially, highlighting the importance of chemical and material management.

Aquatic ecotoxicity follows a similar pattern, led by facilities energy (44.3%) and embedded infrastructure (26.2%), with hot plates (14.6%), sputter tool (6.7%), and oven (2.5%) as notable contributors, showing the role of energy-intensive and solvent-related operations.

Mineral scarcity impacts are primarily driven by embedded facility components (46.1%) and energy consumption (24.4%), with hot plates (12.5%) and the planar sputter tool (10.8%) representing the largest tool-based contributions.

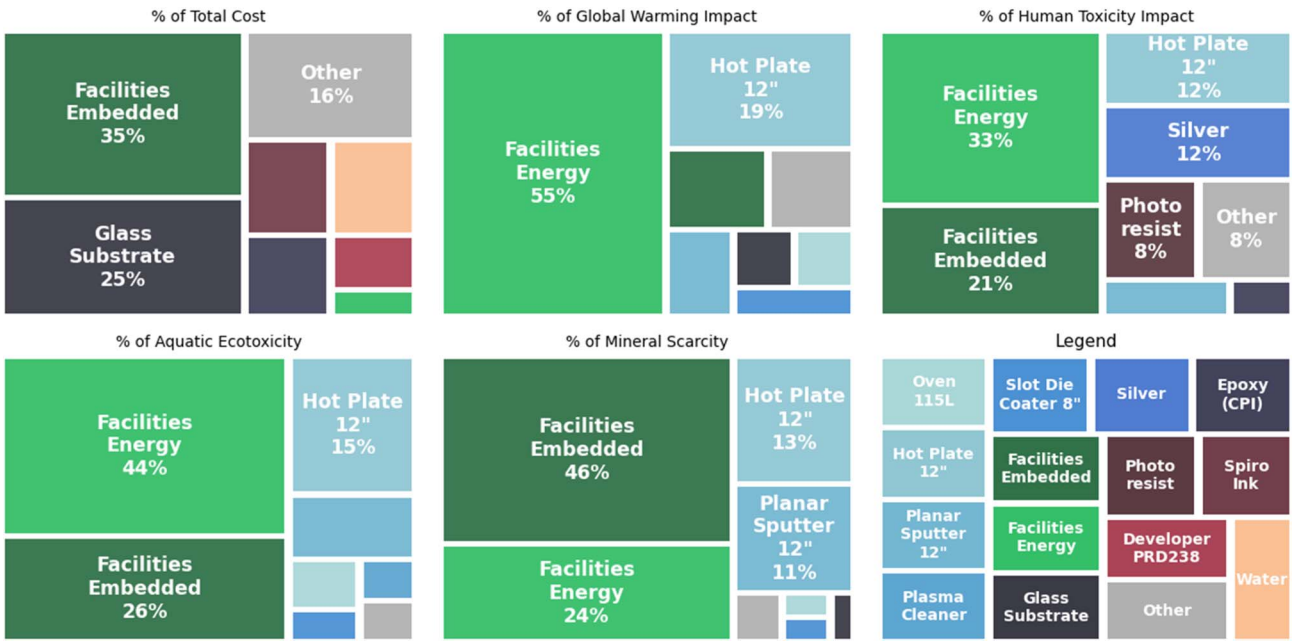

Fig. 5 Proportional contributions of materials, processes, and facility use to environmental impacts in pilot-scale perovskite solar cell manufacturing.

A significant portion of the environmental impacts in this study arises from the operation of electrically powered tools, processing equipment, and supporting facility infrastructure. For example, the hotplates require 3000 W to operate. The pilot-scale perovskite solar cell manufacturing examined here draws electricity from the UK national grid, which, despite decarbonisation efforts, still relies partially on natural gas.

Mitigation of these impacts can follow two main strategies: replacing grid electricity with low-carbon or renewable sources and reducing overall energy use through improved process efficiency. Achieving the latter requires detailed knowledge of the energy demands and operational limits of individual manufacturing steps. The deposition stage, which involves precise temperature control, vacuum environments, and solvent use, is a key target for energy efficiency improvements. Future manufacturing improvements should prioritise lower-temperature processing, reduced vacuum time or higher operating pressures, and the adoption of less harmful solvents.

Pilot-scale manufacturing shows dramatically lower impacts compared with lab-scale production. For 1 m^2 of active area, energy costs at pilot scale are £142.62, compared with £6833 at lab scale. Global warming emissions drop from 7210 kg CO_2-eq. to 150.53 kg CO_2-eq., human toxicity from 1.65 kg 1,4-DCB-eq. to 0.03, aquatic ecotoxicity from 1690 to 37.46, and mineral scarcity from 19.3 to 0.40.

Lab-scale costs exceed £1.65 million per m^2 due primarily to material waste, with global warming impacts reaching 15 995 kg CO_2-eq. and aquatic ecotoxicity over 10.97 kg 1,4-DCB-eq. In contrast, pilot-scale processing reduces costs by 99.8% to £3670 and global warming impacts by 98.9%, highlighting the importance of high-yield production. Energy remains the largest contributor to climate impact, though absolute contributions drop by 98% from lab to pilot scale due to reduced runtime and waste. Embodied emissions decrease by 99% with improved equipment utilisation, and material impacts, while significant in lab-scale and high-defect scenarios, become negligible under optimised conditions.

The difference in dominant impact contributors between laboratory and pilot scale is primarily driven by throughput and allocation effects. At laboratory scale, very low production volumes mean that facility and infrastructure impacts are distributed over a small number of devices, resulting in a high relative contribution from embedded emissions. In contrast, pilot-scale production operates at significantly higher throughput, allowing these impacts to be spread across a much larger number of devices, thereby reducing their relative importance per functional unit.

Energy-intensive equipment, particularly hot plates, contributes significantly at both scales. However, at laboratory scale, impacts from vacuum pump use can exceed those of hot plates due to long processing times and inefficient utilisation. In addition, material-related impacts, particularly from silver, are amplified by higher waste associated with laboratory deposition methods. At pilot scale, improved material efficiency and more continuous operation reduce these effects, shifting the dominant contribution toward overall energy consumption from processing equipment and facilities.

3.3 Enhanced control pilot scale PSC manufacturing

Fig. 6 illustrates an overall reduction across all assessed environmental impact metrics following the implementation of the control system as described in Section 5.2.4. While the control system introduces additional embodied impacts and a small increase in operational energy demand, its overall effect is environmentally beneficial. The added impacts from electronic components are outweighed by reductions in defective production, leading to lower material waste and less need for reprocessing. In addition, improved process stability enables slightly faster production, meaning that time-dependent impacts, such as equipment operation and facility use, benefit from less time in use per device produced. As a result, the per-unit contribution of both machine and building-related impacts is reduced, leading to a net decrease in overall environmental burdens.

Overall global warming impacts are reduced by approximately 10%, total human toxicity by 8%, aquatic ecotoxicity by 8%, and mineral resource scarcity by 7%. These improvements are largely attributable to increased process efficiency, particularly in the deposition stage, where enhanced control reduces the processing time required within cleanroom facilities. As a consequence, overall energy demand is lowered, contributing to the observed environmental gains.

In this updated breakdown of cost contributions Fig. 7, the glass substrate remains the dominant single material cost at 25.4%, with water and epoxy also representing notable fractions. Compared to earlier configurations, the relative cost of energy and embedded facilities remains stable, while material-specific cost shares have shifted slightly, reflecting process adjustments and refinements in input estimation.

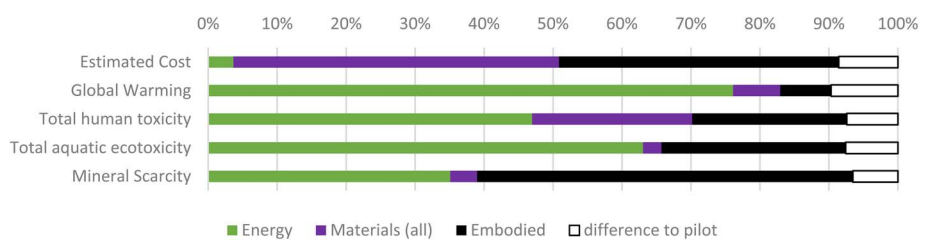

Fig. 6 Breakdown of environmental impacts by energy, materials, and embedded contributions for controlled pilot-scale manufacturing of perovskite solar cells.

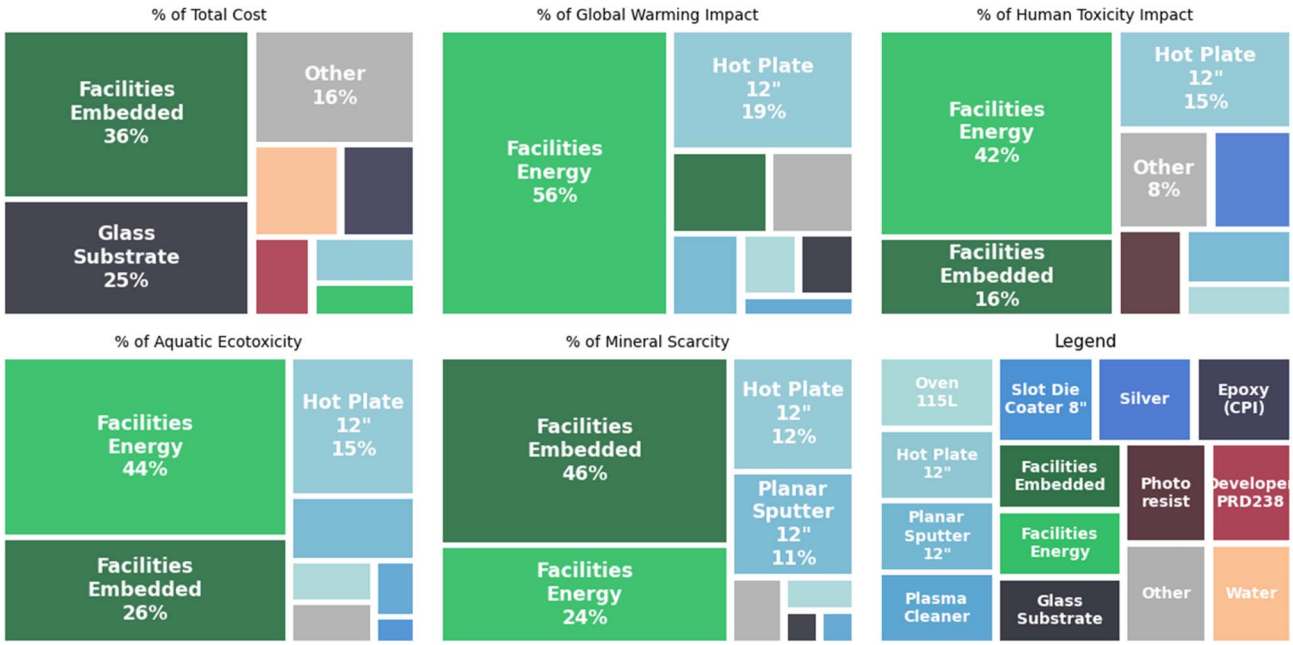

Fig. 7 Proportional contributions of materials, processes, and facility use to environmental impacts in controlled pilot-scale perovskite solar cell manufacturing.

The global warming profile is still dominated by electrically powered equipment, with 12″ hot plates contributing nearly 19% and facilities energy representing over half of the total impact. The updated configuration shows a slight increase in energy's share, likely due to higher operational efficiency or longer runtimes for thermal tools and plasma cleaners.

Human toxicity impacts remain largely influenced by hot plates, contributing 15.1%, while the influence of silver has decreased compared to previous data. Facilities energy continues to dominate at 42%, reflecting the toxicity associated with upstream electricity generation. Minor redistributions among chemical inputs and tools suggest slight changes in material use or improvements in source data accuracy.

Aquatic ecotoxicity is primarily driven by facilities energy and embedded infrastructure, with 12″ hot plates and sputtering tools also contributing significantly. Overall patterns are consistent with earlier results, although small increases in individual tool contributions indicate modest changes in throughput or operational time.

Mineral scarcity is still overwhelmingly affected by embedded facility impacts (46%) and energy (24.3%). Contributions from tools such as planar sputter equipment and hot plates remain stable, while plasma cleaner impacts reflect updated inventory data, suggesting consistent material demand patterns across the system.

The implementation of an advanced control system within the pilot-scale perovskite cell manufacturing process leads to a clear overall reduction in environmental burdens across all assessed impact categories. Although the control system introduces some additional embodied and energy-related emissions due to its integration, the net outcome is beneficial. The results indicate reductions of approximately 10% in global warming potential, 8% in both human toxicity and aquatic ecotoxicity, and 7% in mineral resource scarcity.

These improvements are largely driven by enhanced process efficiency, particularly during the deposition stage. By shortening the processing time required in energy-intensive cleanroom environments, the control system effectively reduces total energy demand. The updated impact tables support these findings, with minor shifts in the relative contributions of thermal tools and facilities energy. Despite some increase in embodied impacts due to the new system, the total

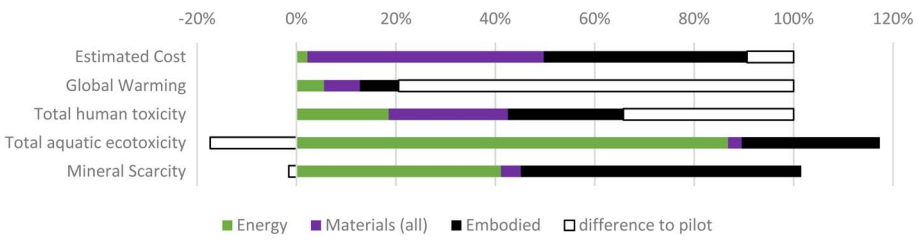

Fig. 8 Breakdown of environmental impacts by energy, materials, and embedded contributions for controlled, wind-powered pilot-scale manufacturing of perovskite solar cells.

environmental performance of the production process is improved. This demonstrates the importance of not only considering the footprint of individual components, but also how integrated process optimisations can yield systemic environmental benefits.

In addition to process optimisation, the study also considers the implications of sourcing electricity from low-carbon energy systems, such as wind power. Given that energy consumption, particularly from electrically powered cleanroom equipment, is a dominant contributor to global warming and other environmental impacts, transitioning to renewable electricity sources could yield substantial further reductions. Preliminary modelling suggests that substituting grid electricity with wind energy could significantly lower the overall carbon footprint, reinforcing the value of both energy efficiency measures and cleaner energy procurement strategies in sustainable device manufacturing.

3.4 Wind powered and enhanced control pilot scale PSC manufacturing

The effect of using more sustainable electrical power substantially changes the impact profile of perovskite cell production, though it is not always positive as shown in Fig. 8. This study has used wind power in the UK as the energy source. Compared to the default pilot-scale study, this reduces costs by 9% and global warming potential by 79%. Total human toxicity decreases by 34%, while mineral scarcity is almost unchanged at −2%. However, aquatic ecotoxicity increases by 17%, meaning the global warming and toxicity benefits must be balanced against increased ecological harm.

The increase in aquatic ecotoxicity is primarily driven by copper use within the upstream infrastructure of wind energy systems. A key contributing factor is the treatment of copper-containing waste, particularly through incineration processes represented in the background database, which generate emissions associated with elevated ecotoxicity impacts.[30] As wind power deployment increases, so too does the demand for copper-intensive components such as generators, cabling, and electrical systems, amplifying these upstream effects.

A potential mitigation pathway lies in improving end-of-life management of copper through reuse and high-quality recycling. Closed-loop recycling systems and reduced reliance on disposal pathways such as incineration could significantly lower associated emissions, thereby reducing aquatic ecotoxicity impacts while maintaining the broader climate benefits of renewable energy integration.

The results in Fig. 9 outlines the distribution of financial costs associated with producing a single perovskite device under improved process conditions. Embedded facility costs remain the largest contributor (36%), followed by the glass substrate (26%) and supporting materials such as water, epoxy, and Spiro ink. Compared to earlier setups, the reduced share of facilities energy costs reflects increased efficiency. Transitioning to wind energy would not significantly affect direct cost figures in this context but could influence the embedded cost structure of grid electricity over time.

Global warming impacts are primarily driven by the glass substrate (15%) and energy-intensive equipment, including hot plates and the use of organic solvents. Embedded facilities continue to contribute substantially (28.9%), although their relative share has declined. Replacing the grid electricity mix with wind-generated power would notably reduce global warming effects, especially from facilities energy (16.7%), enhancing the overall environmental performance of the system.

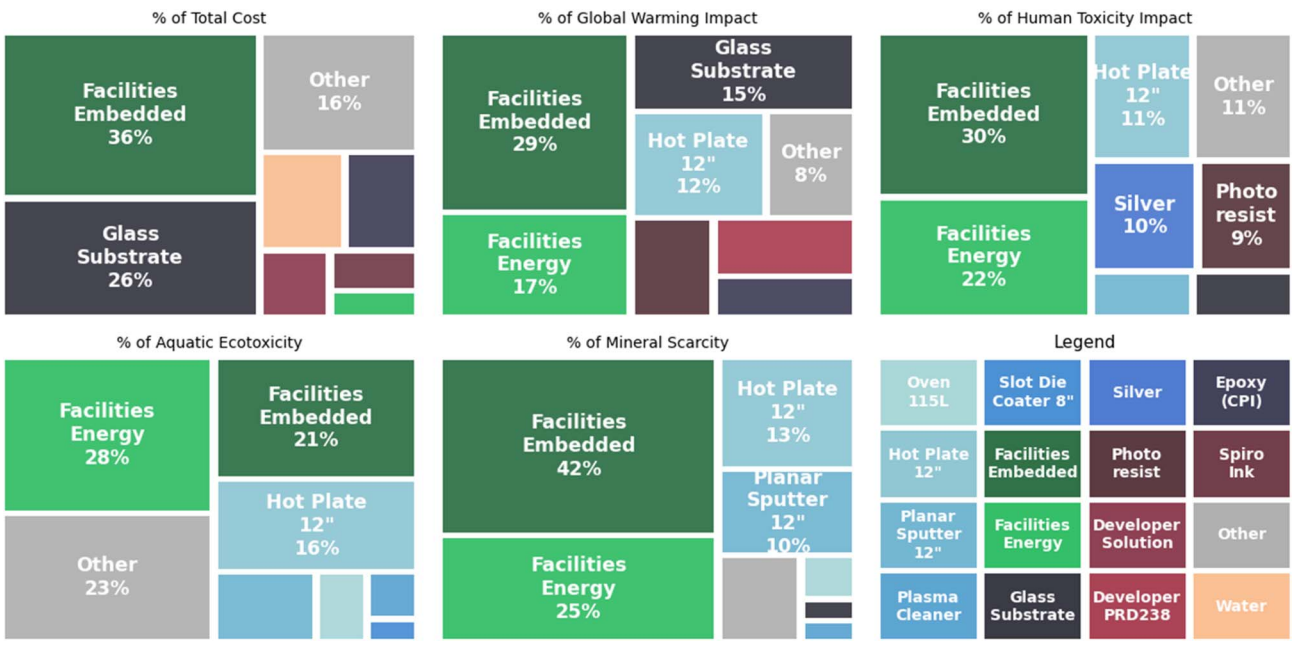

Fig. 9 Proportional contributions of materials, processes, and facility use to environmental impacts in controlled, wind powered pilot-scale perovskite solar cell manufacturing.

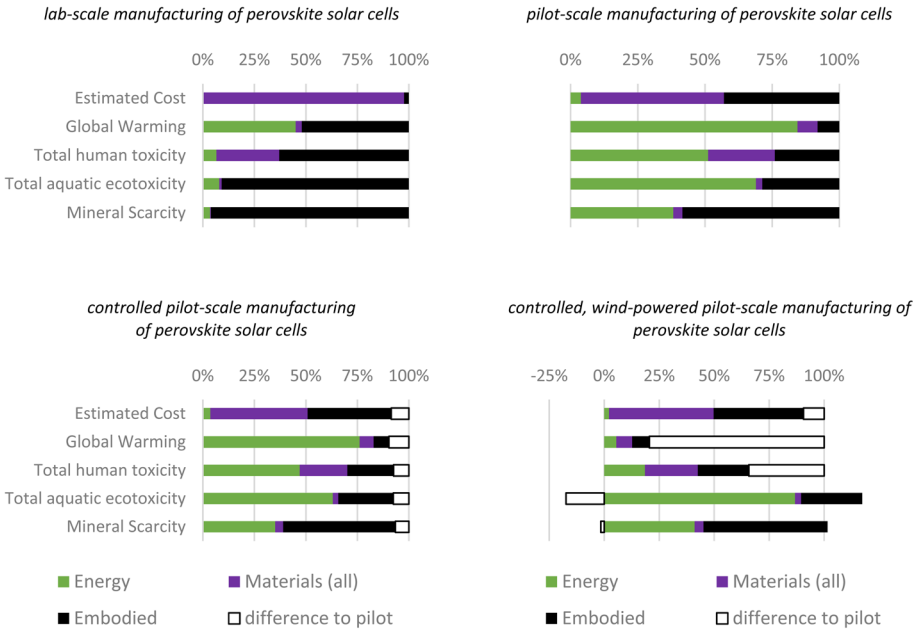

Fig. 10 Breakdown of environmental impacts by energy, materials, and embedded contributions for all tested scenarios.

Toxicity burdens are distributed across facility-related impacts, both embodied (29.6%) and operational energy (21.6%), as well as materials such as silver (9.7%) and photoresist chemicals. Equipment, including hot plates and sputtering tools, also contributes meaningfully. Switching to wind power reduces toxicity associated with electricity generation, particularly benefiting the facilities energy category and lowering total human toxicity by mitigating upstream fossil-fuel emissions.

Ecotoxicity is strongly influenced by equipment use, while embedded facilities and energy account for nearly half of total impacts. Integrating wind energy reduces aquatic ecotoxicity linked to electricity generation, improving energy-related categories and reinforcing the environmental benefits of optimized process design.

Mineral scarcity is dominated by embedded facility emissions (42.0%) and process energy use (25%), with notable contributions from specific tools. While wind energy does not directly affect material-based depletion, it can indirectly reduce mineral scarcity impacts by decreasing the demand for electricity infrastructure and fossil fuel extraction, particularly within the energy category.

The refined production setup demonstrates clear gains in environmental and cost efficiency for single-device perovskite manufacturing. Embedded facility costs remain the dominant cost contributor, but improved process control has reduced energy-related expenditures. Material contributions such as the glass substrate and epoxy remain significant, though more manageable under optimized conditions. Importantly, the use of wind energy, while not altering direct material or device costs, holds potential to reduce upstream energy-related impacts, especially as electricity supply chains decarbonize.

Environmental impacts also reflect these process improvements. Global warming, human toxicity, aquatic ecotoxicity, and mineral scarcity impacts are all more evenly distributed across sources, with a noticeable decrease in the relative contribution of energy and embedded emissions. Equipment and material use still drive key impact categories, but these are now more amenable to mitigation through cleaner energy sources. The integration of wind-generated electricity would further enhance environmental performance, particularly by reducing burdens from electricity-intensive operations and lowering the lifecycle impacts associated with facility energy. This suggests that combining improved process control with renewable energy sourcing offers a clear pathway to more sustainable perovskite device production.

3.5 Summary results

Fig. 10 presents the breakdown of environmental impacts by energy, materials, and embedded contributions across all scenarios, highlighting clear differences in impact profiles. Laboratory scale production is dominated by embedded emissions due to very low throughput, while pilot-scale scenarios show a shift toward energy-driven impacts. The implementation of process control provides consistent but modest reductions across all impact categories. Substituting grid electricity with wind power does not significantly affect costs but substantially reduces global warming potential and human toxicity, with a trade-off of increased aquatic ecotoxicity.

While this study focuses on manufacturing impacts, the full life cycle performance of perovskite solar cells will ultimately depend on operational lifetime, degradation behaviour, and end-of-life management. The substantial reductions in cost and environmental burdens observed at pilot scale highlight the potential of PSCs; however, these benefits must be sustained over sufficiently long device lifetimes to deliver net environmental advantages over competing photovoltaic technologies. Improvements in device

stability are therefore critical to ensure that manufacturing gains translate into meaningful life cycle performance.

The implementation of advanced process control systems offers additional benefits beyond those quantified in this study. In addition to reducing material waste and reprocessing, tighter control over fabrication conditions is likely to improve device quality and consistency. This has two important implications: enhanced energy conversion efficiency and extended operational lifetime. Improvements in either factor reduce life cycle impacts by increasing the total energy generated per unit of environmental burden, effectively distributing manufacturing impacts over a longer and more productive device lifespan. Future work should therefore integrate performance metrics, such as efficiency and degradation rates, into life cycle assessments to better capture these effects.

End-of-life considerations also require further attention to ensure a fully holistic assessment. In particular, the management of metal components and potentially hazardous materials will play a key role in determining overall environmental outcomes. Developing effective recycling and recovery pathways will be essential to minimise resource losses and mitigate toxicity-related impacts.

In parallel, future research should prioritise the replacement of high-impact materials identified in this study, including Spiro-OMeTAD, silver electrodes, and toxic solvents, with lower-impact alternatives. Promising directions include inorganic or carbon-based transport layers, copper or aluminium contacts, and greener solvent systems. These substitutions should be supported by comparative life cycle assessment to ensure that burden shifting is avoided and that material innovations lead to genuine environmental improvements.

4 Conclusions

This study presents a comprehensive cost and environmental life cycle assessment (LCA) of perovskite solar cell production, comparing laboratory-scale research fabrication with pilot-scale manufacturing. The analysis highlights the contributions of materials, energy, and embodied impacts across both scales, revealing strong scale-dependence in both economic and environmental performance.

Scaling from laboratory to pilot production significantly reduces costs and environmental burdens. For 1 m^2 of active area, total costs fall by ~99.8% and global warming emissions decrease by ~98.9%, with comparable reductions in human toxicity, aquatic ecotoxicity, and mineral resource use. These improvements are driven by higher-yield deposition methods at pilot scale, including screen printing and slot-die coating, which reduce material waste, improve throughput, and optimize equipment and facility utilization. At laboratory scale, material inefficiencies dominate costs, while at pilot scale, energy consumption in processing equipment and cleanroom operations becomes the primary environmental driver.

At laboratory scale, low production volumes lead to high per-unit contributions from facility infrastructure, while at pilot scale, higher throughput reduces these effects. Although hot plates are significant at both scales, laboratory impacts are further increased by inefficient vacuum pump use and higher material waste, particularly from silver, whereas pilot-scale impacts are dominated by overall energy consumption.

Enhancing process control further improves sustainability. Implementing automated control systems at the deposition stage reduces processing times, particularly in energy-intensive cleanroom environments, leading to ~10% lower global warming potential, ~8% lower human and aquatic toxicity, and ~7% lower mineral resource scarcity. High-yield production reduces scrap generation, amplifying material and energy efficiency gains. Cost reductions of ~8% also accompany these improvements, demonstrating that targeted process optimizations can yield systemic benefits.

Transitioning to low-carbon electricity, exemplified here by UK wind power, magnifies these gains. Global warming potential is reduced by ~79%, human toxicity by ~34%, and energy-related emissions are substantially mitigated. A minor increase in aquatic ecotoxicity (~17%) arises from upstream renewable infrastructure impacts, illustrating trade-offs in environmental decision-making. Together, enhanced process control and renewable energy integration offer a clear pathway toward low-carbon, high-efficiency perovskite solar cell manufacturing.

Finally, the study underscores the importance of balancing LCA detail with tractability in complex manufacturing systems. Dynamic modelling and process optimization should focus on critical system behaviours and key environmental hotspots to produce actionable insights. Future research should explore deposition efficiency improvements, energy reduction in cleanrooms, alternative lower-impact materials, and broader integration of renewable energy, guiding scalable, cost-effective, and environmentally responsible perovskite production.

Key research priorities include reducing cleanroom energy intensity through process redesign and the transition toward ambient-condition fabrication, thereby lowering the reliance on energy-intensive controlled environments. Improving production yield is also critical and can be achieved through advanced in-line monitoring, defect detection, and enhanced process control, which together minimise waste and reprocessing. In parallel, the integration of low-carbon energy systems at scale will be essential to further reduce operational emissions associated with manufacturing. Finally, the development of high-quality, industry-representative life cycle inventory data is needed to reduce uncertainty and improve the robustness of environmental assessments for emerging photovoltaic manufacturing systems.

Author contributions

Conceptualization: Nathan Dodd, Rachael Rothman, Lenny Koh; methodology: Nathan Dodd, Rachael Rothman, Lenny Koh, Alan Dunbar, David Bird; formal analysis and investigation: Nathan Dodd, Alan Dunbar, David Bird; writing – original draft preparation: Nathan Dodd; writing – review and editing: Nathan Dodd, Rachael Rothman, Lenny Koh, Alan Dunbar, David Bird; funding acquisition: Rachael Rothman; supervision: Rachael Rothman, Lenny Koh.

Conflicts of interest

There is no conflict of interest.

Data availability

The data used in this study are available from the ecoinvent database, version 3.11 (ecoinvent Association, Zurich, Switzerland). Access to the database requires a license, which can be obtained *via* https://ecoinvent.org.

Acknowledgements

For the purpose of open access, the author has applied a Creative Commons Attribution (CC BY) licence to any Author Accepted Manuscript version arising. The research leading to these results received funding from EPSRC under Grant Agreements EP/V051261/1 and EP/W018950/1. The authors would like to acknowledge the contributions of; Ian Ross and Jonathan Howse for their efforts, time and help in aiding the execution of this work.

References

1 C. Yang, W. Hu, J. Liu, C. Han, Q. Gao, A. Mei, *et al.*, Achievements, challenges, and future prospects for industrialization of perovskite solar cells, *Light: Science and Applications*, Springer Nature, 2024, DOI: 10.1038/s41377-024-01461-x.

2 A. Kojima, K. Teshima, Y. Shirai and T. Miyasaka, Organometal halide perovskites as visible-light sensitizers for photovoltaic cells, *J. Am. Chem. Soc.*, 2009, **131**(17), 6050–6051, DOI: 10.1021/ja809598r.

3 National Laboratory of the Rockies (NLR), 2025, Best Research-Cell Efficiency Chart, https://www.nrel.gov/pv/cell-efficiency.

4 J. A. Alberola-Borràs, J. A. Baker, F. De Rossi, R. Vidal, D. Beynon, K. E. A. Hooper, *et al.*, Perovskite Photovoltaic Modules: Life Cycle Assessment of Pre-industrial Production Process, *iScience*, 2018, **9**, 542–551, DOI: 10.1016/j.isci.2018.10.020.

5 Y. Rahaq, M. Moussa, A. Mohammad, H. Wang and A. Hassan, Highly reproducible perovskite solar cells via controlling the morphologies of the perovskite thin films by the solution-processed two-step method, *J. Mater. Sci.: Mater. Electron.*, 2018, **29**(19), 16426–16436, DOI: 10.1007/s10854-018-9734-4.

6 S. Razza, S. Pescetelli, A. Agresti and A. Di Carlo, Laser processing optimization for large-area perovskite solar modules, *Energies*, 2021, **14**(4), DOI: 10.3390/en14041069.

7 X. Tian, S. D. Stranks and F. You, Life cycle energy use and environmental implications of high-performance perovskite tandem solar cells [Internet], 2020, available from: https://www.science.org.

8 S. Bello, A. Urwick, F. Bastianini, A. J. Nedoma and A. Dunbar, An introduction to perovskites for solar cells and their characterisation, *Energy Rep.*, 2022, **8**, 89–106, DOI: 10.1016/j.egyr.2022.08.205.

9 M. Roffeis, S. Kirner, J. C. Goldschmidt, B. Stannowski, L. M. Perez, C. Case, *et al.*, New insights into the environmental performance of perovskite-on-silicon tandem solar cells - a life cycle assessment of industrially manufactured modules, *Sustainable Energy Fuels*, 2022, **6**(12), 2924–2940, DOI: 10.1039/d2se00096b.

10 T. Okoroafor, A. Maalouf, S. Oez, V. Babu, B. Wilk and S. Resalati, Life cycle assessment of inkjet printed perovskite solar cells, *J. Cleaner Prod.*, 2022, 373, DOI: 10.1016/j.jclepro.2022.133665.

11 E. Leccisi and V. Fthenakis, Life cycle energy demand and carbon emissions of scalable single-junction and tandem perovskite PV, *Prog. Photovoltaics*, 2021, **29**(10), 1078–1092, DOI: 10.1002/pip.3442.

12 I. Celik, Z. Song, A. J. Cimaroli, Y. Yan, M. J. Heben and D. Apul, Life Cycle Assessment (LCA) of perovskite PV cells projected from lab to fab, *Sol. Energy Mater. Sol. Cells*, 2016, **156**, 157–169, DOI: 10.1016/j.solmat.2016.04.037.

13 M. Wong-Stringer, *Optimisation of Fabrication Processes for Stable and Scalable Perovskite Solar Cells*, 2018.

14 B. Kang and F. Yan, Emerging strategies for the large-scale fabrication of perovskite solar modules: from design to process, *Energy Environ. Sci.*, 2025, 3917–3954, DOI: 10.1039/d4ee05613b.

15 Z. Zhang, Q. Sun, Y. Lu, F. Lu, X. Mu, S. H. Wei, *et al.*, Hydrogenated Cs2AgBiBr6 for significantly improved efficiency of lead-free inorganic double perovskite solar cell, *Nat. Commun.*, 2022, **13**(1), DOI: 10.1038/s41467-022-31016-w.

16 G. Carcano, M. Ceriani and F. Soglio, Spin Coating with High Viscosity Photoresist on Square Substrates-Applications in the Thin Film Hybrid Microwave Integrated Circuit Field [Internet], DOI: 10.1108/eb044507, available from https://www.emerald.com/mi/article-pdf/10/3/12/1988674/eb044507.pdf.

17 fomtechnologies, slot-die coating in the future of photovoltaics, 2025, https://www.fomtechnologies.com/insights-blog/the-role-of-slot-die-coating-in-the-future-of-photovoltaics.

18 F. Yang, D. Jang, L. Dong, S. Qiu, A. Distler, N. Li, *et al.*, Upscaling Solution-Processed Perovskite Photovoltaics, *Adv. Energy Mater.*, 2021, DOI: 10.1002/aenm.202101973.

19 Masruroh, G. A. Maulana, I. M. Syarifuddin, F. O. R. Sukma, M. A. Hanif, G. Saroja, *et al.*, Tuning Viscosity and Spin Time to Enhance the Thinnest rGO Film Coating in SPR Sensors, *Plasmonics*, 2025, **20**, 6105–6114, DOI: 10.1007/s11468-025-03110-4.

20 R. Patidar, D. Burkitt, K. Hooper, D. Richards and T. Watson, Slot-Die Coating of Perovskite Solar Cells: An Overview, 2020, DOI: 10.1016/j.mtcomm.2019.100808Getrightsandcontent.

21 D. Burkitt, R. Patidar, P. Greenwood, K. Hooper, J. McGettrick, S. Dimitrov, *et al.*, Roll-to-roll slot-die coated P-I-N perovskite solar cells using acetonitrile based single step perovskite solvent system, *Sustainable Energy Fuels*, 2020, **4**(7), 3340–3351, DOI: 10.1039/d0se00460j.

22 P. Roy, N. Kumar Sinha, S. Tiwari and A. Khare, A review on perovskite solar cells: Evolution of architecture, fabrication techniques, commercialization issues and status, *Sol. Energy*, 2020, 665–688, DOI: 10.1016/j.solener.2020.01.080.
23 N. Giovanni, D. Lupo and G. Simone, *Organic and Printed Electronics : Fundamentals and Applications*, Pan Stanford Publishing, 2016, p. 580.
24 S. Ahmad, *Perovskite Solar Cells: Materials, Processes, and Devices*, Wiley-VCH, 2021, pp. 348–432.
25 N. Espinosa, L. Serrano-Luján, A. Urbina and F. C. Krebs, Solution and vapour deposited lead perovskite solar cells: Ecotoxicity from a life cycle assessment perspective, *Sol. Energy Mater. Sol. Cells*, 2015, **137**, 303–310, DOI: 10.1016/j.solmat.2015.02.013.
26 T. Ibn-Mohammed, S. C. L. Koh, I. M. Reaney, A. Acquaye, G. Schileo, K. B. Mustapha, *et al.*, Perovskite solar cells: An integrated hybrid lifecycle assessment and review in comparison with other photovoltaic technologies, *Renewable Sustainable Energy Rev.*, 2017, 1321–1344, DOI: 10.1016/j.rser.2017.05.095.
27 J. Gong, S. B. Darling and F. You, Perovskite photovoltaics: Life-cycle assessment of energy and environmental impacts, *Energy Environ. Sci.*, 2015, **8**(7), 1953–1968, DOI: 10.1039/c5ee00615e.
28 M. A. Scarpulla, B. McCandless, A. B. Phillips, Y. Yan, M. J. Heben, C. Wolden, *et al.*, CdTe-based thin film photovoltaics: Recent advances, current challenges and future prospects, *Sol. Energy Mater. Sol. Cells*, 2023, DOI: 10.1016/j.solmat.2023.112289.
29 D. Bird, *Conversations with David Bird CPI*, 2024.
30 *ecoinvent. ecoinvent 3.8 Dataset Documentation "electricity production, wind, >3MW turbine, onshore-GB-electricity, high voltage"*, 2021.